Electric resistivity during electrodialytic recovery of phosphorous from sewage sludge ash

Ottosen, Lisbeth M.; Lima, Ana T.

Published in:
Case Studies in Chemical and Environmental Engineering

Link to article, DOI:
10.1016/j.cscee.2021.100092

Publication date:
2021

Document Version
Publisher's PDF, also known as Version of record

Case Studies in Chemical and Environmental Engineering 3 (2021) 100092

Contents lists available at ScienceDirect

Case Studies in Chemical and Environmental Engineering

journal homepage: www.editorialmanager.com/cscee/default.aspx

Electric resistivity during electrodialytic recovery of phosphorous from sewage sludge ash

Lisbeth M. Ottosen *, Ana T. Lima

Department of Civil Engineering, Technical University of Denmark, 2800, Lyngby, Denmark

ARTICLE INFO

Keywords:
Electric resistivity
Membrane resistivity
Chemical gradients
Phosphorous recovery
Sewage sludge ash

ABSTRACT

This paper focuses on changes in potential drops over different parts of a two-compartment electrodialtyic cell during a process developed for P recovery from sewage sludge ash and simultaneous removal of heavy metals. The cell has two compartments separated by a cation exchange membrane. The ash suspension is in the anode compartment. The major aim of this work is to obtain knowledge needed to optimize the energy consumption for the process. Initially, a low conductivity of the suspension caused a relatively high resistance in the suspension itself. The adjacent catholyte contrast with a high conductivity and a low pH. A high membrane resistivity was seen because of the concentration and pH gradients. During the treatment, the gradients leveled out and, the overall voltage reached a low level. However, at this point, where the suspension is acidic, protons are major current carriers, which is a waste of energy to the overall recovery process, since current should be spent to transport metal cations across the membrane. Thus, the investigation points at two major issues for future optimization; the gradients over the cation exchange membrane (pH, conductivity, potential) and improved utilization of the produced protons to be for P extraction rather than carrying current.

1. Introduction

Electro-membrane processes are membrane-based electrochemical separation processes in which ion-exchange membranes and electrical potential are used to separate ionic species from aqueous solution and other uncharged components [1]. The driving force for the flux of ion in electro-membrane processes is a gradient of electrochemical potential [1]. The present paper uses electrodialytic recovery (EDR), an electro-membrane process developed for simultaneous recovery of phosphorous and separation of heavy metals from sewage sludge ash (SSA). The process targets to separate the SSA into resources: a clean P product for industrial use [2–4] and a particulate fraction, which can be utilized in construction materials [5,6]. Different other techniques are under development for recovery of P from SSA. The techniques can be grouped in two: thermochemical treatment or chemical extraction. These methods are reviewed in Ref. [7]. A major challenge with the wet extraction is the simultaneous extraction of heavy metals and P [8]. In order to obtain a clean P, various additional processes to the wet extraction for separation of P and heavy metals have been suggested: pH adjustment [9,10], sulfide precipitation [9] and cation exchange [9,11]. EDR is a one-step process where the P extraction and heavy metal separation occur simultaneously [2].

The principle of the two-compartment EDR is illustrated in Fig. 1. The SSA suspension is in the anode compartment and a cation exchange membrane (CEM) separates the two compartments. When applying the DC current, the electrical conductance is converted to ionic conductance at the electrode/electrolyte interfaces, and the SSA suspension will gradually acidify due to electrolysis of water at the anode ($H_2O \rightarrow 2H^+ + ½O_2$ (g) + $2e^-$). During the acidification, heavy metals and P are extracted from the SSA, but whereas the cationic heavy metal are transported by electromigration over the CEM and concentrate in the cathode compartment, the extracted P remains in the liquid phase of the ash suspension as negatively charged ions or neutral molecules [2]. Hereby simultaneous extraction and separation is obtained, and the CEM plays central role in this separation.

Membranes are central to electrodialysis but present a series of limitations. Because of the physical-chemical separation of membranes, the ion flux across the membrane is strongly influenced by the boundary layer formed at the membrane/solution interface [12]. The boundary layer thickness is a function of velocity and flow spacer geometry, and it may be minimized by promoting turbulent flow, and thus increasing the limiting current density [13]. The SSA suspension is constantly stirred in EDR which may minimize the thickness of the boundary layer, but as

* Corresponding author.
E-mail address: LO@byg.dtu.dk (L.M. Ottosen).

https://doi.org/10.1016/j.cscee.2021.100092
Received 6 September 2020; Received in revised form 15 February 2021; Accepted 17 February 2021

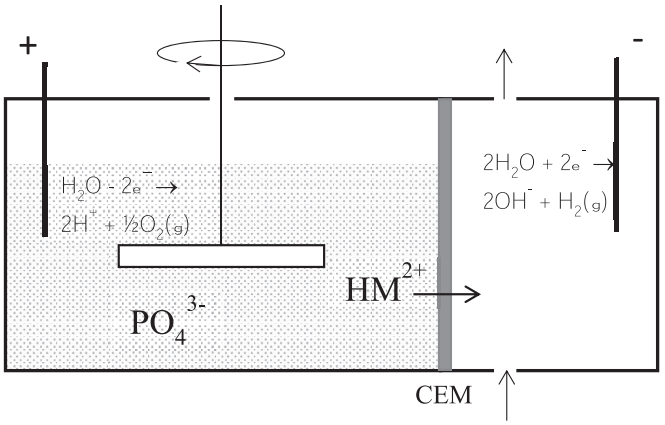

Fig. 1. The principle of EDR. The SSA is gradually acidified from the protons produced from the electrode process at the anode. P and heavy metals (HM) are desorbed and HM are electromigrating into the catholyte.

pointed out by authors dealing with electrodialysis systems, if turbulence does not reach membrane surface, laminar flow prevails and limiting current density is reduced significantly [12]. This implies a polarization effect. Concentration polarization at the surface of the CEMs are well recognized in literature [14]. But, because electrodialysis in general occurs in flow systems, static, steady-state polarization build-up at CEMs surface – which is the case in the EDR cell – has not yet been investigated.

This paper looks to study resistivity over the EDR cell during the process. EDR is driven by electrical power, and thus the power consumption is of major importance to the cost for running the process. Power is the product of voltage and current, and the power consumption is the power per unit of time. As a constant current is applied during the EDR experiments, the voltage is determined by the electrical resistivity over the cell (Ohms law) – the higher the resistivity the higher the voltage. The major objective of the present paper is to understand electrical resistivity fluctuations in the cell and across the CEM, both spatially (within the cell) and temporal (with advancement of experimental time). In order to optimize EDR and minimize power consumption, it is crucial to understand the changes during EDR and to identify the major contribution to the overall resistivity. A new experimental setup was developed for this work. The EDR cell was equipped with three electrodes in the anode compartment placed at different distances to the CEM (Fig. 2). When measuring current-voltage relations between each of these three electrodes as anodes and the cathode, it is possible to distinguish between

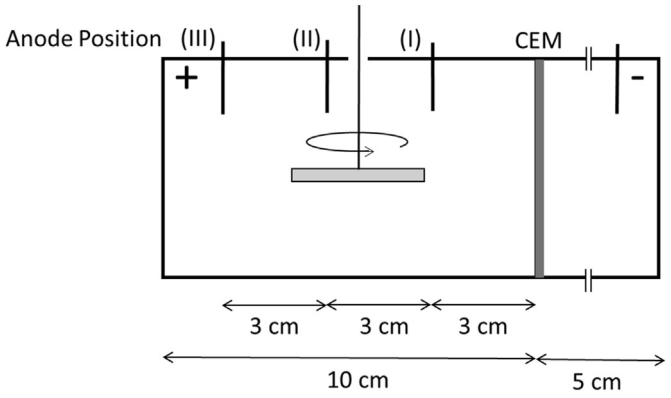

Fig. 2. Schematic presentation of the EDR laboratory cell where the SSA is kept suspended by stirring in the anode compartment. The anode can have three positions (I-III). A cation exchange membrane (CEM) separates the two compartments.

the resistivity in the anolyte and over the rest of the cell including the CEM. A movable anode was previously suggested when measuring membrane resistance as a means to eliminate the contribution of the electrolyte by extrapolation [15] and used here with the same intent – only the anode is not movable but fixed at different positions. A constant current is used in EDR because the extraction of P depends on the proton production from electrolysis at the anode, which again depends on the applied current.

The novelty of this paper is the developed setup and the increased understanding of the resistivity changes during EDR in the different parts of the cell. Especially, the new setup allows following the spatial and temporal changes in membrane resistance as result of continuous changes in the conductivity in the electrolytes at each side of the membrane. In literature, the resistance of ion exchange membranes is most often determined in a standard solution (0.5 M NaCl), but it depends strongly on the solution concentration [16]. Thus, the new setup enables new details on the changing membrane resistance during electrodialtyic processes.

2. Potentials across the two-compartment EDR cell

The direct current in the EDR cell is applied perpendicular to the membrane. The EDR experiments are conducted at a constant current mode, and thus changes in resistivity in the different parts of the cell during the experiments result in changes in potential differences (Ohms law). Fig. 2 offers a schematization of potential gradients across the two-compartment EDR cell used in this study. The EDR cell operates with constant stirring in the SSA suspension/anolyte (2) and circulating of the catholyte (4) (Fig. 2). For this reason, no build up of concentration gradients are considered in these compartments i.e. there are constant potential drops. The potential drops are considered dependent on their respective conductivities, i.e. concentration and type of ions. The potential drops over electrode surfaces (1) and (5) are influenced by polarization, which is the inevitable process responsible for extra and nonproductive energy consumption. The standard potential for water oxidation reaction at the anode ($E^\circ = -1.229$ V) and at the cathode ($E^\circ = -0.828$ V) are the minimum potentials applied to pass a current. Higher potentials may be necessary for current to flow, as the processes are kinetically controlled, and this extra need corresponds to the overpotential. The overpotential can be divided into many different subcategories, and the major overpotentials are eliminated in the EDR cell by choosing the platinum-coated titanium electrodes and the stirring/circulating of the suspension/catholyte. The potential drop over the membrane (3) is influenced by concentration polarization. Concentration polarization occurs in all membrane separation processes owing to differences in the transport numbers of ions in the solution and in the ion exchange membrane [17]. In EDR as shown in Fig. 1, the concentration of cations at the surface of the CEM in the SSA suspension is reduced compared to in the suspension because of the higher transport number of cations in the CEM. Electro-neutrality requirements means that this is an overall reduction of the electrolyte concentration in this boundary layer, and a concentration gradient is established between the membrane surface and the SSA suspension. On the cathode side of the CEM, the electrolyte concentration at the membrane surface is increased accordingly. The potential drop over the CEM includes the potential drop over the membrane itself and over these boundary layers. Current–voltage curves reflect the relationship between the current (and voltage) across a membrane and the adjacent boundary layers, thus providing information about the resistance of the system against ion transport [16]. Current-voltage curves are generally used to distinguish three regions [18]. In the first region (at low current densities), the ohmic region, there is a linear relationship between current and voltage over the membrane. When the limiting current density is reached, the curve reaches a plateau value (second region). The third part of the curve, the overlimiting region is the region where electro-convection occurs.

3. Materials and methods

3.1. The two-compartment EDR cell and experiments

The EDR laboratory cell (Fig. 2) was made from Plexiglas, with an internal diameter of 8 cm. It consisted of two compartments – a cathode compartment and an anode compartment. The compartments were separated by a cation exchange membrane (CEM) from IONICS (3009753). The cathode was in a fixed position, while the anode could have 3 positions; 3, 6 and 9 cm from the CEM. The electrodes were made of platinum coated titanium wire (diameter 3 mm) obtained from Permascand® and the length of the anode in the SSA suspension was approximately 20 cm (winded around). The power supply was Hewlett Packard E3612A. In the cathode compartment, 500 ml 0.01 M NaNO3 adjusted to pH 2 with HNO_3 was circulated. The circulation of the catholyte ensures a continuous flow in this compartment that removes the produced H_2 gas from the electrolysis out of the compartment.

The SSA was suspended in tap water with pH at 7.4 to 7.7 and a conductivity of 0.8 mS/cm. Experiments were made with liquid:solid (L:S) ratios of 3.5, 7 and 14. In every experiment the SSA was suspended in 350 ml water and the L:S ratio was adjusted by the mass of SSA (100 g, 50 g or 25 g dry SSA, respectively). The SSA was kept suspended by an overhead stirrer (RW11 basic from IKA).

During the experiments, daily samples of about 10 ml were taken from the catholyte. In these samples, pH was measured, where after the sample was poured back into the catholyte. The pH in the catholyte was then manually adjusted to between 1 and 2 with 1:1 HNO_3 (the pH was controlled by measurement 30 min after the adjustment). At the same time, samples were taken from the SSA suspension, and in these the pH and conductivity were measured with Radiometer electrodes. The samples were purred back after measurements. In experiment A4, the pH and conductivity were measured several times a day during the experiments to closely follow the changes.

Four EDR experiments were carried out with SSA-A and 2 with SSA-B (Table 1). An overview of the performed EDR experiments are in Table 1. The experiments were conducted at a constant current of 50 or 75 mA applied between the cathode and the anode in position II (Fig. 1b). The duration of all experiments was 1 week. At the end of the EDR experiments the suspension was filtered. Contents of P, Cu and Zn were measured in the SSA, solutions, cation exchange membrane and on the cathode. The contents in the CEM were measured after extraction in 1.0 M HNO_3 for 24 h. Rinsing of the cathode prior to measurement was done in 5.0 M HNO_3 for 24 h.

3.2. Current-voltage measurements

During the EDR experiments, the influence from electrode distance and current on the voltage between the working electrodes was found by a screening process. The procedure was to increase the current from 30 mA → 50 mA → 75 mA → 100 mA and the resulting voltage was noted between the working electrodes at each current. In every experiment, the first screening was 10–20 min after the experiment was started (noted as 15 min hereafter in this paper). After the Screening procedure, the anode connection was returned to position (II) and the original current of the experiment (Table 1) was applied again. The screening procedure took about 20–30 min each time. The power supply was operating in a constant current mode between the cathode and anode II all through the experiments, except for the screening periods where the current was adjusted manually to the different levels at each of the three anodes. The screening was conducted each day of the experiments, but the reported results are limited to 15 min and 7 days, since the conclusions can be drawn from these two screenings. In the first experiments conducted, the current was decreased again (same values backwards) between each of the three anodes and the cathode, and as the voltage stabilized at the same level as when the current was increased, the following experiments were conducted with the increased order only.

In experiment A4, in which the pH changes and conductivity were followed closely, the 15 min screening was made in an equivalent experiment in order not to have the many screening influencing the pH and conductivity measurements in the suspension.

Table 1
The electrodialytic P recovery experiments.

Experiment number	SSA (g)	L/S ratio	Current (mA)	Screening 30-50-75-100 mA
A1	25	14	50	15 min and 7 days
A2	50	7	50	15 min and 7 days
A3	100	3.5	50	15 min and 7 days
A4	50	7	75	15 min and 7 days
B1	50	7	50	15 min and 7 days
B2	50	7	75	15 min and 7 days

3.3. Investigated SSAs and characterization

Experiments were carried out with two different SSAs obtained from mono-incineration plants where municipal sewage sludge is incinerated in fluidized-bed. One from Germany (named SSA-A) and one from BIOFOS-Avedøre, Denmark (named SSA-B).

Concentrations of P, Cu and Zn were measured after pre-treatment of the ash in accordance to Danish Standard DS259; 1.0 g ash and 20.0 ml (1:1) HNO_3 was heated at 200 kPa (120 °C) for 30 min. Filtration through 0.45 μm filter and the concentrations in the filtrate were measured with a Varian 720-ES ICP-OES (Inductively Coupled Plasma-Optical Emission Spectrometry). Ash pH and conductivity were measured by suspending 10.0 g ash in 25 ml distilled water. After 1 h agitation and few minutes of setting, pH and conductivity were measured directly in the suspension with Radiometer electrodes. The suspension was filtered, followed by measurement of Cl^- and SO_4^{2-} concentrations by Ion Chromatography (Thermo Scientific Dionex ICS-1100) giving the water soluble concentrations. Loss on ignition (LoI) was found after 30 min at 550 °C. Water content was measured as weight loss after 24 h at 105 °C (calculated as weight loss over the weight of the wet sample). Five to six replicates of each of these analyses were made. Solubility in water was evaluated: 50.0 g ash suspended in 500 ml distilled water and agitated for 1 min. After settling, the water was decanted. New 500 ml distilled water added. This was repeated so the ash was washed three times. Finally, the suspension was filtered and the ash dried at 105 °C and weighed, and the solubility was then calculated as the percentage of lost weight. The water solubility was measured in two replicates.

4. Results and discussion

4.1. SSA characterization

The SSAs had distinct reddish colors due to the use of Fe to precipitate P at the wastewater treatment plants. Sewage sludge is incinerated at 800–900 °C in excess air and therefore metals are likely to exist as oxides

Table 2
Selected characteristics of the two ashes. Concentrations from Ref. [19] for municipal SSA are given for comparison.

	SSA-A	SSA-B	[19]
pH	9.8 ± 0.01	11.4 ± 0.2	
Conductivity (mS/cm)	3.8 ± 0.05	3.0 ± 0.5	
Loss on Ignition (%)	0.6 ± 0.02	0.3 ± 0.005	
Water content (%)	0.2 ± 0.04	0,3 ± 0.2	
Water solubility (%)	1.9	1.4	
Water soluble Cl^- (mg/kg)	33 ± 3	300 ± 5.9	
Water soluble SO_4^{2-} (mg/kg)	2920 ± 75	5450 ± 136	
P (g/kg)	92 ± 4.2	91.8 ± 1.5	36–131
Cu (mg/kg)	2090 ± 90	490 ± 3	162–3467
Zn (mg/kg)	2490 ± 127	2160 ± 34	552–5515

in the SSA [11], and the reddish color indicate iron-oxides. Table 2 shows some characteristics for the two SSAs. The characteristics were similar for the two ashes, except for the Cu concentration, which was almost 4 times higher in SSA-A than SSA-B (Table 2). The P concentrations were at the same level in the two ashes: SSA-A (92 g P/kg) and SSA-B (90 g P/kg). Krüger et al. (2014) [19] reported concentrations between 36 and 131 g P/kg for German municipal SSAs. The P concentrations in both SSAs of the present investigation are within these limits (Table 2). In addition, the concentrations of Cu and Zn in both the investigated SSAs are also within the ranges reported in Ref. [19], see Table 2. Thus, these concentrations in the investigated SSAs are within the expected range, and the SSAs can be considered representative for SSAs in general in this sense.

4.2. EDR results overview

Table 3 gives an overview of pH and conductivity measured in the SSA suspension the initially (after 15 min) and final (just before terminating the experiments after 7 days). In Table 3 is also the total mass of SSA dissolved during the EDR experiments and the corresponding dissolved percentage in relation to the initial mass as well as the final P concentration in the SSA and the total percentage of P recovered.

4.3. Conductivity and pH in the two cell compartments

The initial conductivity of the catholyte was between 7.1 and 7.5 mS/cm, and pH was 2. Initially, the SSA suspensions had about 3–4 times lower conductivities when compared to the original catholyte (Table 3). This implies a gradient in conductivity over the CEM in the beginning of the experiments. Initially, there was also a pH gradient over the CEM as the suspension was in the neutral region (Table 3) and the pH of the catholyte was about 2.

The pH in the catholyte and the voltage between anode II and cathode during experiment A4 are presented in Fig. 3a, whereas the changes in conductivity and pH in the SSA suspension of the same experiment are in Fig. 3b. The fluctuations in catholyte pH are the result of water electrolysis at the cathode, where pH increases to up to 12 and the daily adjustment to pH 1.5–2.0. The pH fluctuations in the catholyte do not affect the pH in the SSA suspension (Fig. 3b) because the CEM hinders OH^- ions from hydrolysis of water at the cathode to entering the suspension. On the contrary, the fluctuations in catholyte pH strongly influences the overall voltage, which increases with increasing pH. This suggests that there is fouling/precipitation at the CEM when pH increases to neutral and alkaline levels, or that there is precipitation of hydroxides in the catholyte, decreasing the electrolyte ionic concentration. After acidifying the catholyte, these precipitates/fouling products are dissolved and the voltage decreases again. Overall, the pH fluctuations decreases over time and so do the voltage throughout the experiment. The decrease in pH fluctuations is likely linked to the acidification of the SSA suspension, as at acidic pH protons carry current from the suspension into the catholyte, neutralizing the hydroxyl ions produced by the cathode process. Also the increased ion content in the catholyte may influence the voltage fluctuations, since some of these ions (e.g. K^+ and Na^+) probably remains in solution at high pH, so the conductivity in the catholyte

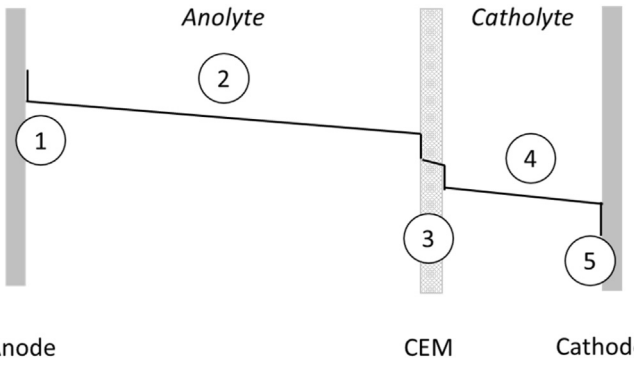

Fig. 3. Potential drops contributing to the voltage between the working electrodes. (1) and (5) are potential drops at the surface of the electrodes; (2) and (4) correspond to the voltage variations across the media placed in the anode and cathode compartments; and (3) is the potential drop across the cation exchange membrane.

reaches a level where it is high enough to maintain a low voltage even at high pH. The overall decrease in voltage over time during the experiments means that the power consumption for the process is highest initially, and that it is within these first days of EDR that an optimization should first focus. As the fluctuations in catholyte pH are seen linked to the overall voltage fluctuations, future research should explore the option to keep catholyte pH constant by continuous titration rather than one daily adjustment.

Water electrolysis at the anode continuously supply protons to the SSA suspension. After 2 days of experiment, pH in the suspension decreases to about 2. The subsequent increase of the suspension conductivity follows a linear pattern up to 35 mS/cm (Fig. 3b). Electrolysis of water at the anode is the desired oxidation reaction here. Possible dissolved anions present in the suspension are attracted to the anode, e.g. SO_4^{2-}, which is presented in a quite high concentration (Table 2), but they do not participate in the anode reaction because they are in their highest oxidation state already in the SSA. The Cl^-, on the other hand, may compete with H^+ formation at the anode in this kind of systems [20], but Cl^- concentration is low (Table 2). Oxidation of Fe^{2+} to Fe^{3+} could potentially also be a relevant electrode process at the anode, but Fe is again present in the SSA at the highest oxidation level (hematite has been identified in other SSAs e.g. Ref. [9]). Thus, water electrolysis is by far the major anodic reaction in the system.

4.4. Electrode distance and resistivity (periodical screening)

The results from the screening after 15 min and after 7 days for experiment A3 three anodes are shown in Fig. 4(a) and (b), respectively, as relation between the anode position (as distance from CEM) and the voltage.

The relation between anode distance from CEM and voltage is linear. The linear correlation in Fig. 4 is evident as R^2 is between 0.989 and 0.992 after 15 min, and between 0.993 and 1.000 after 7 days. The equations and R^2 for the other experiments are to be found in the supplementary material to this article. In every experiment and for all the

Table 3
Summary of SSA main data before and after EDR experiments (Cond = conductivity, dissolved = dissolved SSA, and P_{Final} = P concentration in SSA after EDR).

	SSA suspension				SSA			
	$pH_{Initial}$	pH_{Final}	$Cond_{Initial}$ (mS/cm)	$Cond_{Final}$ (mS/cm)	Dissolved SSA (g)	Dissolved SSA (%)	P_{Final} (g/kg)	P recovered (%)
A1	7.0	1.5	1.2	20.2	10	39	40.1 ± 0.6	65
A2	7.2	1.8	1.8	20.2	14	28	69.5 ± 2.6	42
A3	7.1	1.9	3.4	13.8	14	14	86.2 ± 1.2	17
A4	7.1	1.3	1.8	32.8	22	44	31.3 ± 0.5	74
B1	7.2	1.9	1.4	17.5	15	30	47.7 ± 1.5	53
B2	7.4	1.5	1.8	25.7	21	41	20.9 ± 0.2	73

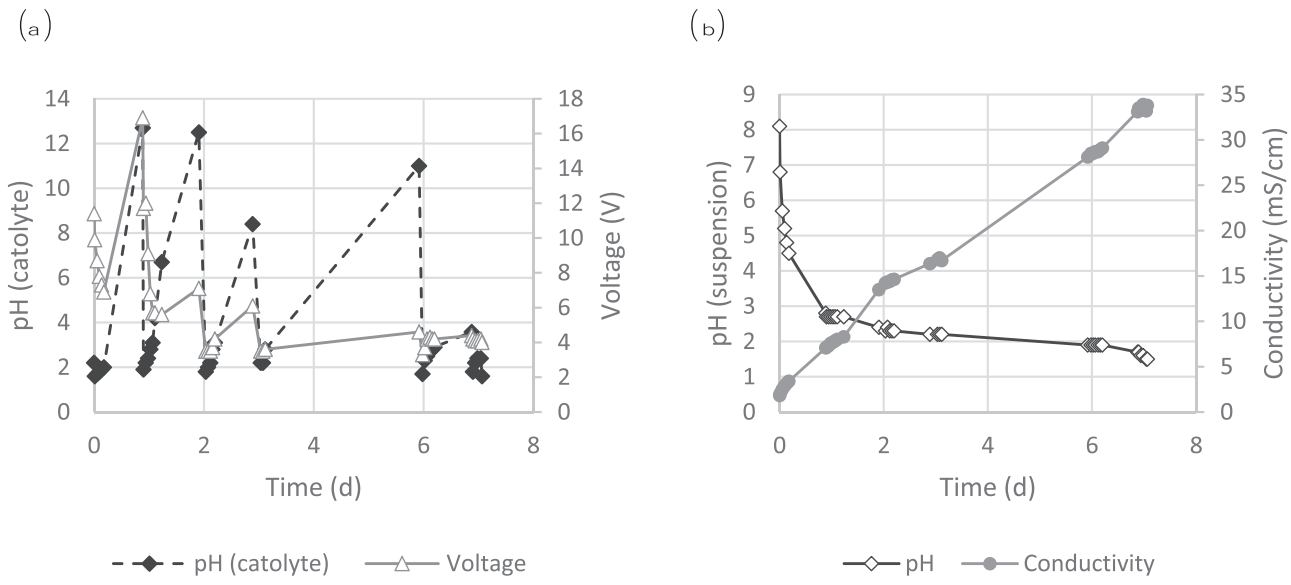

Fig. 4. Experiment A4 (a) pH in the catholyte and voltage between working electrodes, and (b) pH and conductivity in SSA suspension.

tested currents, a linear relation was found similarly to the one presented in Fig. 4 (R^2 between 0.964 and 0.998 after 15 min, and between 0.75 and 1.00 after 7 days). The lower R^2 for few of the equations after 7 days is related to the very small differences in voltage between the different anodes and the cathode (<1 V) and the accuracy of the measurements not being sufficient at these low voltages.

The linear equations constants ($y = ax + b$) gives important information on the current-voltage relation in the EDR cell. The slope of the curves (equation constant *a*) describes the rate at which voltage increases with increasing distance between cathode and anode. Since distance is the only parameter changing between the measurements for each current, the slope *a* equals to the voltage over the suspension in [V/cm] (i.e. the slope of potential drop (2), Fig. 3). The constant *b* represents the voltage in case the anode was placed infinitely close to the CEM where the suspension is stirred (i.e. at the border of the boundary layer). To describe the effects of applied current on the potential gradients in the EDR cell, the relations of *a* and *b* are explored in the next two paragraphs, respectively.

4.4.1. Ohmic drop in SSA suspension

The potential gradient over the suspension (the linear equation constant *a*) is calculated to a resistivity [Ω·cm] using Ohms law for the different applied currents and the voltage measured. Fig. 5(a and b) shows the resistivity of SSA suspension in the used EDR cell as function of the applied current after 15 min and 7 days, respectively. It is seen that for every experiments, the resistivity at each time is independent of the current (the small variations are not systematic and relates to the uncertainties of the measurements).

The resistivity over the stirred SSA suspension reflects how conductive (or resistant) the suspension is. A simplified equation of this relation

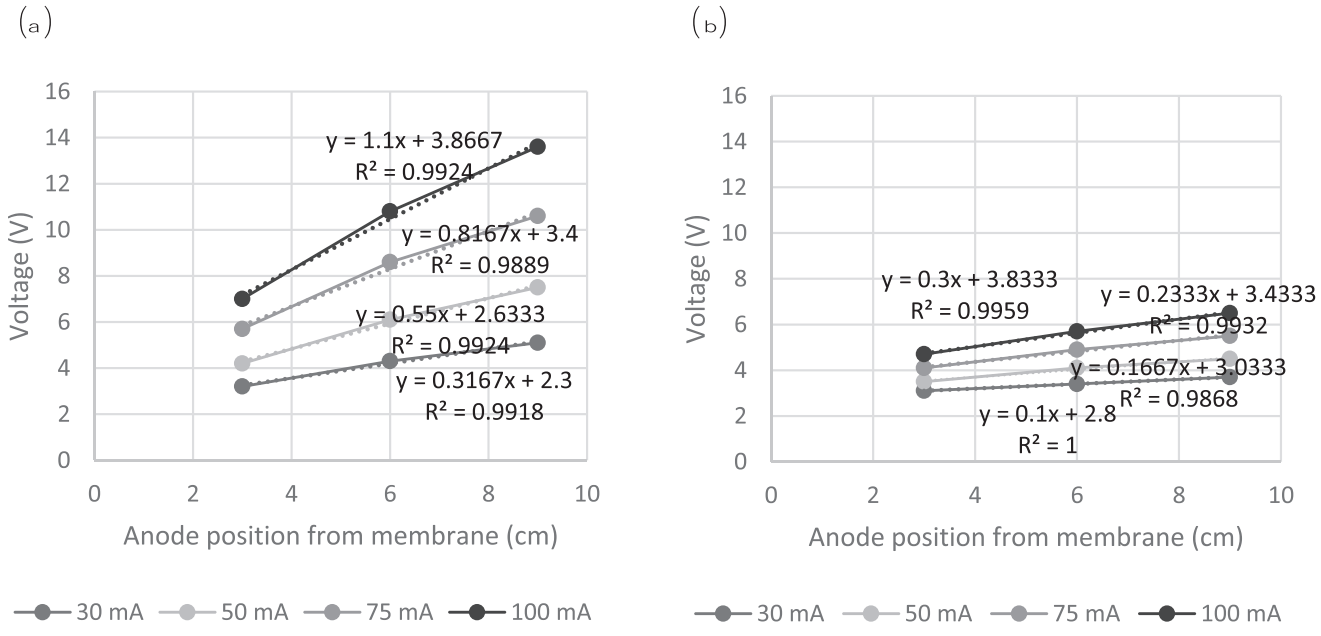

Fig. 5. Experiment A3. Voltage as function of anode position and applied current (a) after 1 h and (b) after 7 days.

can be found in Lima et al. [21] where the length of the sample and cross sectional area are written as a function of sample resistivity (or conductivity). The differences in resistivity after 15 min (Fig. 5a) relates to the differences in L:S ratio, and as seen, the higher the amount of SSA, the lower the resistivity. This again relates to the solubility of the SSA (Table 2) and the following increase in conductivity when suspending a higher SSA mass (comparing experiment A1 to A3 in Table 3). Experiments A2 and A4 are similar to B1 and B2, differing on the type of used SSA, and it is seen that the resistivity per cm after 15 min is higher in experiments with SSA-B (Fig. 7a). This is reasonable since SSA-B has the lowest solubility (Table 2). The SSA suspension resistivity in experiment B2 is about 100 Ω cm less than in B1 even though the SSA and L:S ratio were the same. In experiment B2 the applied current was higher than in experiment B1, and during the 15 min before the measurement was taken the higher production of protons by electrolysis at the anode already gave a slightly lower resistivity in B2. The same goes for experiments A2 and A4, and this shows how fast the resistivity decreases in the beginning of these experiments.

The SSA suspension resistivity decreased significantly from start to after 7 days of EDS (Fig. 5a and b), correlating well to a general decrease in pH (Fig. 5b) and increase of suspension conductivity (Table 3). After 7 days, the resistivity locates between 50 and 100 Ω cm regardless the initial L:S ratio or current applied, except from experiment A3, where it was 150–170 Ω cm. From Table 3 it can be seen that the conductivity in the SSA suspension was the lowest in experiment A3, and that the smallest percentage of SSA was dissolved (corresponding well to this experiment having the highest mass of SSA). This suggests that the produced protons are still consumed for dissolution of SSA in these experiments to a higher extent than in the other experiments. Since H^+ has a higher ionic velocity than the cations released from the SSA during EDR, it must be expected that H^+ ions gives a major contribution to the total charge transfer in the suspension under acidic conditions. In EDR it is relevant to distinguish between the two roles of the protons (I) current carrying and (II) reacting with the particulate material [22]. Using the basis of reactive and current carrying protons in the EDR experiments from the present investigation can explain why experiment A3 differs from the other in a higher resistivity after 7 days. The relation of reactive protons to current carrying protons is different with more reactive protons due to the higher mass of SSA treated. The relation between reactive and current carrying protons needs to be addressed in optimizing EDR. The current carrying protons are contributing to an overall lower resistivity, but they are not as such involved in the P extraction and heavy metal separation during the process as the reactive protons.s

4.4.2. *Current-voltage relations over CEM*

The constant *b*, found from Fig. 4 and appended material, is related to the different screening currents in Fig. 6. *b* represents the potential drop in case the anode was placed infinitely close to the CEM, i.e. the potential drops (1–5) from Fig. 2 excluding the potential drop (2) over the SSA suspension. The potential drop (*b* constant) is dependent on the applied current – the higher the current the higher the *b*. Similar to the *a* constant (the resistivity of the SSA suspension) (Fig. 5) the initial differences of the *b* constant were leveled out after 7 days (Fig. 6). Analyzing the pattern after 15 min reveals that the higher the amount of suspended SSA (and therefore the higher the suspension conductivity), the lower the *b* constant, even though the potential drop over the SSA suspension is not included in the *b* constant. This illustrates the importance of the CEM on the overall process efficiency. The potential drop over the CEM, i.e. the membrane resistance, is an important parameter affecting power consumption in electrodialytic processes [23]. In fact, the transport of cations through the CEM is believed to be the rate controlling step and thus responsible for the major energy consumption in EDR of soil in a packed column [22].

In most literature, it is assumed that the membrane resistance is independent of the electrolyte concentration and corresponds to the value determined in a standard solution (0.5 M NaCl) [16]. However, the resistance of ion exchange membranes strongly depends on the solution concentration, and especially at low solution concentrations (<0.1 M NaCl) [16]. In the EDR cell used in the current investigation, the conductivity in the SSA suspension was measured to 1.2–3.4 mS/cm initially (Table 3). Compared to the conductivity of 0.1 M NaCl (which is 10.6 mS/cm), the SSA suspension has such a low initial conductivity, so it must influence the membrane resistance in accordance to the findings of [16]. In addition, there was an initial conductivity gradient over the CEM, as the conductivity in the catholyte was 7.1–7.5 mS/cm initially, i.e. a factor of 2–6 times the conductivity of the catholyte compared to

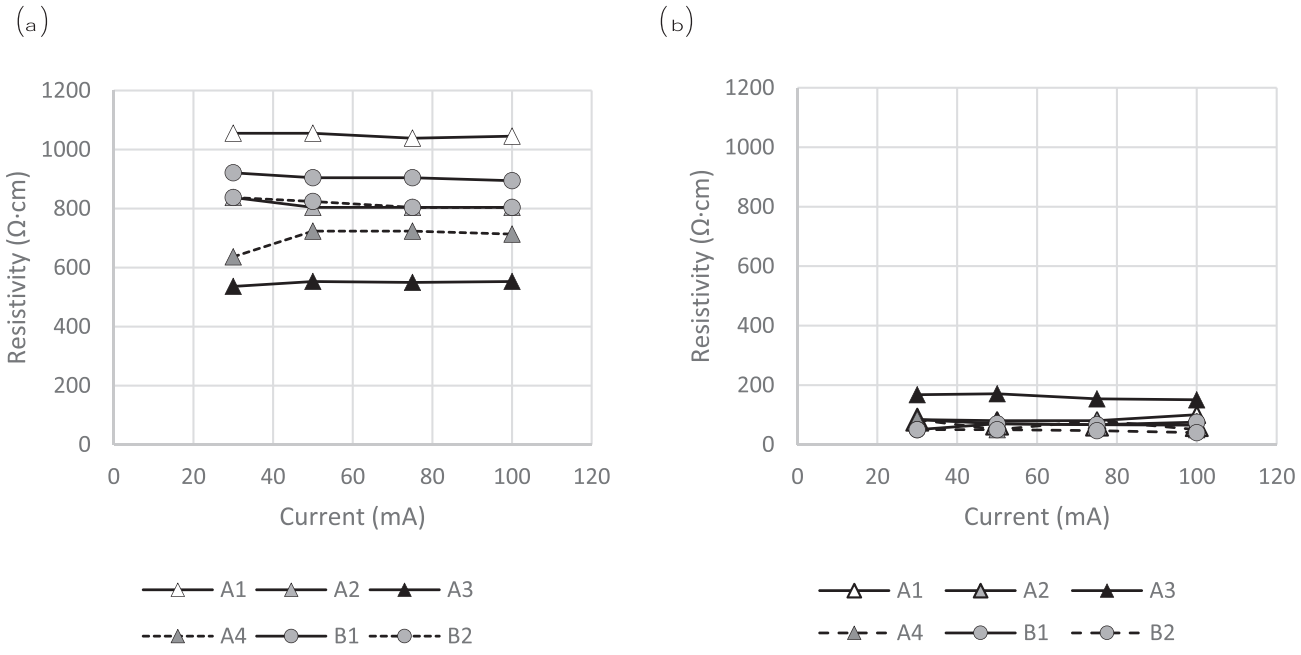

Fig. 6. Relation between resistivity (equation constant a Fig. 5 divided by the current and multiplied by the cell cross section area) and the current in the SSA suspension after (a) 15 min and (b) 7 days.

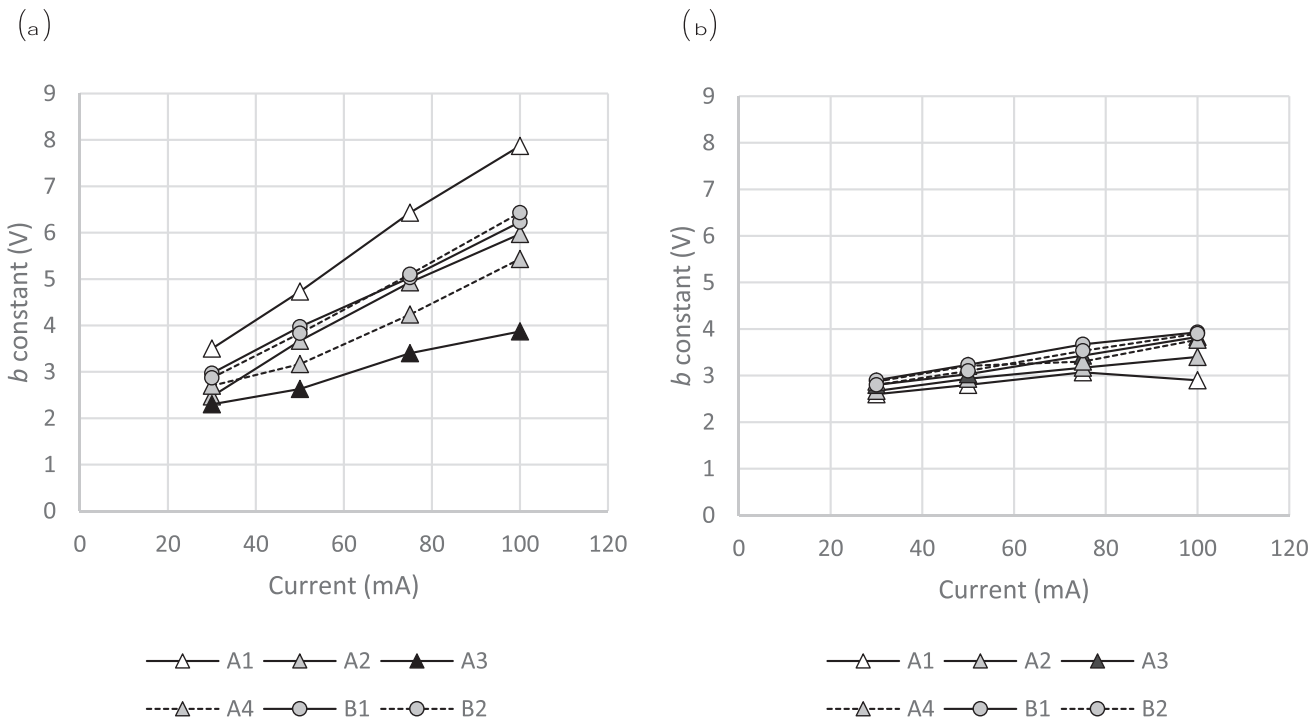

Fig. 7. Potential drop over EDR cell excluding the potential drop over SSA suspension (equation constant b, Fig. 4) after (a) 15 min and (b) 7 days.

the SSA suspension. Geise et al. [24] showed that a concentration gradient over a CEM, where the concentration was highest in the feed (1.0 M NaCl) and lowest in the catholyte (0.01 M NaCl), resulted in a higher resistivity over the CEM compared to the same concentration (1.0 M NaCl) at both sides of the membrane. The results in the present paper underlines that the membrane resistance is highly influenced by the changes in concentrations during EDR, and that it cannot be considered independent of the electrolyte concentrations.

At day 7 of the experiments, the differences in the *b* constant are very small for the different applied currents (Fig. 6b). When applying 30 mA during the screening, the difference in all the b constants for the different EDR experiments was only 0.3 V (2.6–2.9 V, see Supplementary material) and the accuracy of the measurements is not sufficient to evaluate the differences in the b constants as after 15 min. The major conclusion is here that the electrical resistivity in the suspension is low and that the *b* constants after 7 days at the applied currents (Table 1) were between 2.6 and 3.9 V (Supplementary material).

4.5. Electrodialytic separation results

The mass of P, Cu and Zn (in mg) distributed in the SSA, filtrate and cathode compartment at the end of the experiments are shown in Fig. 8. The mass in the cathode compartment is a sum of the mass electrodeposited at the cathode, dissolved in the catholyte and adsorbed in the CEM. The mass balance is defined as the sum of masses of a chemical element in all the different parts at the end of the experiment relative to the initial mass of the same chemical element in the SSA (based on the average initial concentration). In heterogeneous particulate samples as SSA, the mass balances for EDR samples varies around 100%. Below the experiment number in Fig. 8, the mass balances for the different experiments are found. In general, the mass balances for P and Zn are between 90 and 110%, which is regarded as acceptable for EDR treatments of environmental samples; for Cu on the other hand, the mass balances show more variability (83–122%). As there is not systematics in high and low mass balances for the different elements, the differences are likely linked to the samples taken for measurement of initial concentrations not being representative for the whole SSA batch used in these experiments. The P recovery is calculated as the P content in the liquid phase of the suspension divided by the total content found in all the different parts at the end of the experiment. The highest P recovery was in experiments A4 and B2, and here it was 73–74%, which is lower than the previously obtained 80%–90% [2–4], but the experimental conditions were also different.

In every experiment, the extracted P was mainly in the filtrate and the extracted Cu and Zn in the catholyte, and thus the separation occurred as intended. A very similar P mass was extracted in the experiments with the same SSA and same current A1, A2 and A3 (50 mA), but different L:S. This corresponds to the total mass loss of the SSAs also being at the same level 10–14 g at 50 mA. From experiment B1 at the same current, 15 g was dissolved. The dissolved mass was 21 and 22 g from SSA-A and SSA-B at 75 mA, respectively (Table 3). Thus, increasing the current from 50 mA to 75 mA increased the SSA dissolution accordingly with about 1/3. Overall, the recovered percentage of P follows the suspension dissolution (see Table 3). Table 3 also shows the pH and conductivity of the SSA suspension at the end of the EDS experiments. The pH is lowest in the experiments with 75 mA (A4 and B2) and the conductivity highest. A general pattern for the experiments A1 to A3 is that the less SSA in the cell, the lower pH. In the directly comparable experiments with SSA-A and SSA-B (A2-B1 and A4-B2) SSA-B has the highest pH, and thus there are difference when treating the two different SSAs. However, the overall P recovery achieved from the two ashes are very similar to comparable experiments. The separation of Cu and Zn was successful in that the major part of the extracted Cu and Zn was transported to and kept in the cathode compartment in every experiment. This is in accordance to previously reported findings [2–4] and it underlines the ability to have a simultaneous P extraction and heavy metals separation when treating SSA by EDR.

5. Conclusions

This work focused on the changes influencing P extraction and overall resistivity during electrodialytic recovery. Fluctuations in

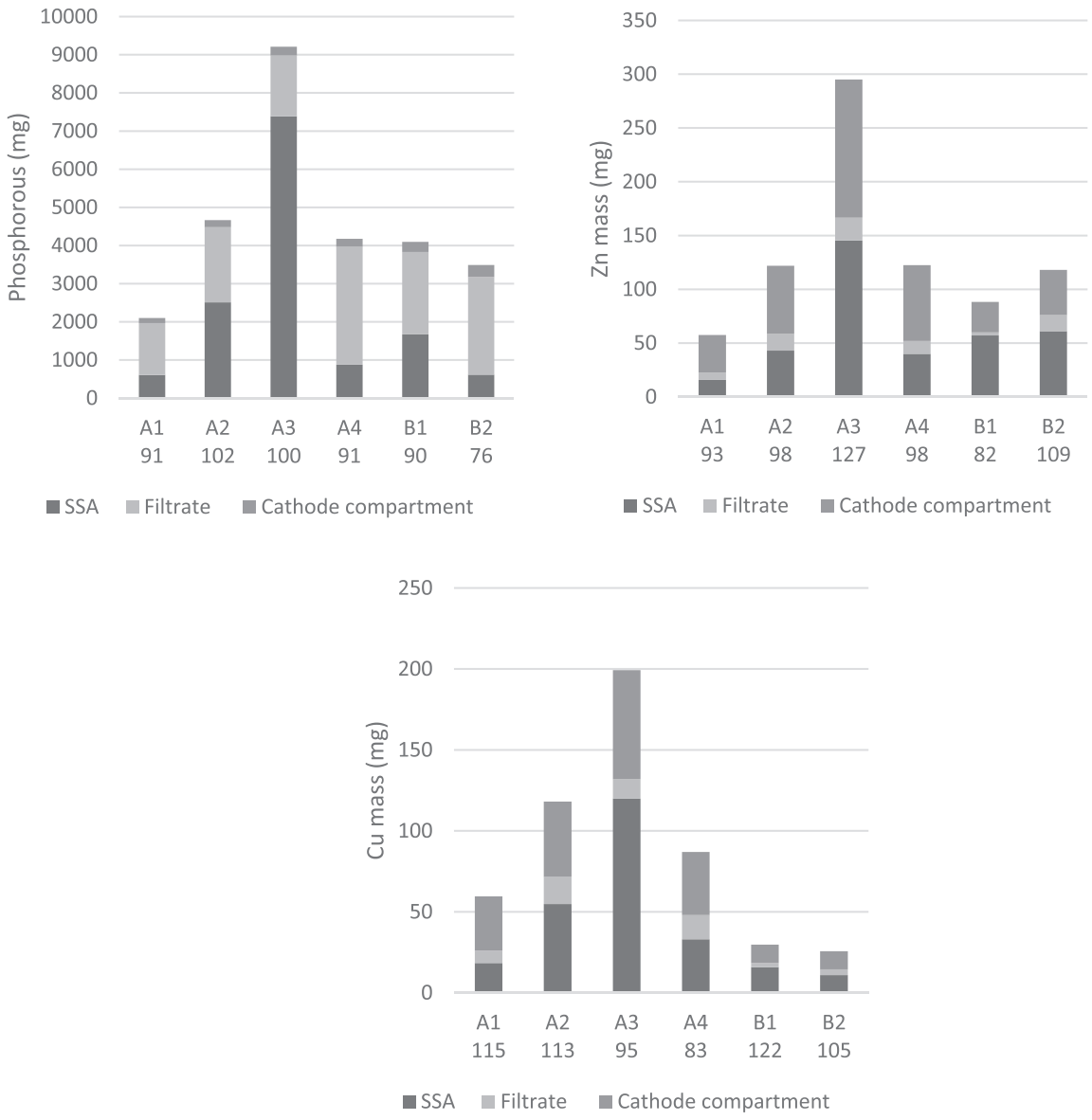

Fig. 8. Distribution of (a) P, (b) Zn and (c) Cu in the EDR cell by the end of the experiments. The mass balance is given below the name of the experiment in the x-axis. What is shown as in cathode compartment is a sum of mass found in CEM, catolyte and on cathode.

catholyte pH strongly influenced the overall voltage but not the pH and conductivity in the SSA suspension (placed in the anode compartment). In the measurements after 15 min of EDR, the liquid-to-solid ratio of the SSA suspension strongly influenced the overall voltage as the more SSA suspended the more dissolved phase. The mass of SSA suspended directly influenced the resistivity of the suspension itself but also the resistivity of the cation exchange membrane. Conductivity and pH gradient over the membrane were considered to be responsible to the high membrane resistivity. After 7 days, the conductivity in the SSA suspension was high and the overall cell voltage accordingly at a low level. The protons produced in the SSA suspension by water electrolysis at the anode extracts the P. At the same time, the protons will also be major charge carriers when the suspension is acidified, resulting in a lower overall voltage/resistivity, but also in a waste of current in transporting protons from anode to cathode compartment. Thus, mutual optimization of liquid–to-solid ratio and current is an important future task.

Declaration of competing interest

The authors declare that they have no known competing financial interests or personal relationships that could have appeared to influence the work reported in this paper.

Acknowledgements

The research leading to these results partially received funding from the European Union's Horizon 2020 research and innovation program under the Marie Sklodowska-Curie grant agreement no. 713683 (COFUNDfellowsDTU).

Appendix A. Supplementary data

Supplementary data to this article can be found online at https://doi.org/10.1016/j.cscee.2021.100092.

References

[1] M. Kumar, M.A. Khan, Z.A. Al-Othman, T.S.Y. Choong, Recent developments in ion-exchange membranes and their applications in electrochemical processes for in situ ion substitutions, separation and water splitting, Separ. Purif. Rev. 42 (2013) 187–261, https://doi.org/10.1080/15422119.2012.690360.

[2] L.M. Ottosen, P.E. Jensen, G.M. Kirkelund, Phosphorous recovery from sewage sludge ash suspended in water in a two-compartment electrodialytic cell, Waste Manag. 51 (2016) 142–148, https://doi.org/10.1016/j.wasman.2016.02.015.

[3] B. Ebbers, L.M. Ottosen, P.E. Jensen, Comparison of two different electrodialytic cells for separation of phosphorus and heavy metals from sewage sludge ash, Chemosphere 125 (2015) 122–129, https://doi.org/10.1016/j.chemosphere.2014.12.013.

[4] P. Guedes, N. Couto, L.M. Ottosen, G.M. Kirkelund, E. Mateus, A.B. Ribeiro, Valorisation of ferric sewage sludge ashes: potential as a phosphorus source, Waste Manag. 52 (2016) 193–201, https://doi.org/10.1016/j.wasman.2016.03.040.

[5] A. Kappel, R.P. Viader, K.P. Kowalski, G.M. Kirkelund, L.M. Ottosen, Utilisation of electrodialytically treated sewage sludge ash in mortar, Waste and Biomass Valorization 9 (2018) 2503–2515, https://doi.org/10.1007/s12649-018-0215-z.

[6] L.M. Ottosen, I.M.G. Bertelsen, P.E. Jensen, G.M. Kirkelund, Sewage sludge ash as resource for phosphorous and material for clay brick manufacturing, Construct. Build. Mater. 249 (2020), 118684.

[7] S. Donatello, C.R. Cheeseman, Recycling and recovery routes for incinerated sewage sludge ash (ISSA): a review, Waste Manag. 33 (2013) 2328–2340, https://doi.org/10.1016/j.wasman.2013.05.024.

[8] H. Herzel, O. Krüger, L. Hermann, C. Adam, Sewage sludge ash - a promising secondary phosphorus source for fertilizer production, Sci. Total Environ. 542 (2016) 1136–1143, https://doi.org/10.1016/j.scitotenv.2015.08.059.

[9] M. Franz, Phosphate fertilizer from sewage sludge ash (SSA), Waste Manag. 28 (2008) 1809–1818, https://doi.org/10.1016/j.wasman.2007.08.011.

[10] M. Takahashi, S. Kato, H. Shima, E. Sarai, T. Ichioka, S. Hatyakawa, H. Miyajiri, Technology for recovering phosphorus from incinerated wastewater treatment sludge, in: Chemosphere, Pergamon, 2001, pp. 23–29, https://doi.org/10.1016/S0045-6535(00)00380-5.

[11] S. Donatello, A. Freeman-Pask, M. Tyrer, C.R. Cheeseman, Effect of milling and acid washing on the pozzolanic activity of incinerator sewage sludge ash, Cement Concr. Compos. 32 (2010) 54–61, https://doi.org/10.1016/j.cemconcomp.2009.09.002.

[12] Y. Tanaka, Chapter 2 electrodialysis reversal, Membr. Sci. Technol. 12 (2007) 383–404, https://doi.org/10.1016/S0927-5193(07)12016-7.

[13] J.M. Chiapello, M. Bernard, Improved spacer design and cost reduction in an electrodialysis system, J. Membr. Sci. 80 (1993) 251–256, https://doi.org/10.1016/0376-7388(93)85149-Q.

[14] Y. Tanaka, Water dissociation in ion-exchange membrane electrodialysis, J. Membr. Sci. 203 (2002) 227–244, https://doi.org/10.1016/S0376-7388(02)00011-X.

[15] F.L. Ramp, A method of characterizing ion-exchange membranes by conductance measurements, Desalination 16 (1975) 321–329, https://doi.org/10.1016/S0011-9164(00)88005-4.

[16] P. Długołecki, B. Anet, S.J. Metz, K. Nijmeijer, M. Wessling, Transport limitations in ion exchange membranes at low salt concentrations, J. Membr. Sci. 346 (2010) 163–171, https://doi.org/10.1016/j.memsci.2009.09.033.

[17] H. Strathmann, Chapter 6 ion-exchange membrane processes in water treatment, Sustain. Sci. Eng. 2 (2010) 141–199, https://doi.org/10.1016/S1871-2711(09)00206-2.

[18] R. Ibanez, D.F. Stamatialis, M. Wessling, Role of membrane surface in concentration polarization at cation exchange membranes, J. Membr. Sci. 239 (2004) 119–128, https://doi.org/10.1016/j.memsci.2003.12.032.

[19] O. Krüger, A. Grabner, C. Adam, Complete survey of German sewage sludge ash, Environ. Sci. Technol. 48 (2014) 11811–11818, https://doi.org/10.1021/es502766x.

[20] J.M. Paz-García, B. Johannesson, L.M. Ottosen, A.B. Ribeiro, J.M. Rodríguez-Maroto, Simulation-based Analysis of the Differences in the Removal Rate of Chlorides, Nitrates and Sulfates by Electrokinetic Desalination Treatments, 2013, https://doi.org/10.1016/j.electacta.2012.11.087.

[21] A.T. Lima, J.P.G. Loch, P.J. Kleingeld, Bentonite electrical conductivity: a model based on series–parallel transport, J. Appl. Electrochem. 40 (2010) 1061–1068, https://doi.org/10.1007/s10800-009-0060-7.

[22] T.R. Sun, L.M. Ottosen, J. Mortensen, Electrodialytic Soil Remediation Enhanced by Low Frequency Pulse Current - Overall Chronopotentiometric Measurement, 2013, https://doi.org/10.1016/j.chemosphere.2012.08.038.

[23] A.H. Galama, D.A. Vermaas, J. Veerman, M. Saakes, H.H.M. Rijnaarts, J.W. Post, K. Nijmeijer, Membrane resistance: the effect of salinity gradients over a cation exchange membrane, J. Membr. Sci. 467 (2014) 279–291, https://doi.org/10.1016/j.memsci.2014.05.046.

[24] G.M. Geise, A.J. Curtis, M.C. Hatzell, M.A. Hickner, B.E. Logan, Salt concentration differences alter membrane resistance in reverse electrodialysis stacks, Environ. Sci. Technol. Lett. 1 (2014) 36–39, https://doi.org/10.1021/ez4000719.